Appendix A

Imaging Data

Table A.1: Sample images of the galaxies in NGC 4065 group in B, V, R_C and [SII] filters

No.	Name	*B*	*V*	R_c	SII
1	NGC 4070	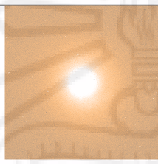	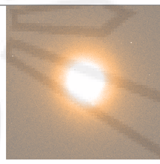	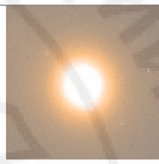	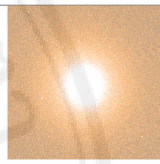
2	J12040831+2023280	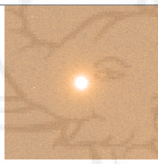	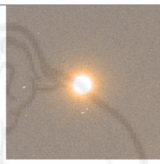	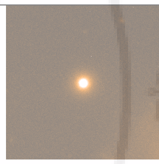	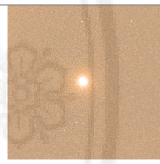
3	NGC 4066	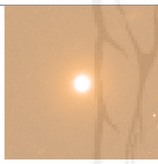	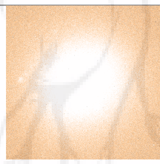	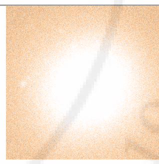	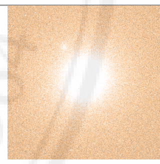
4	NGC 4069	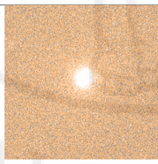	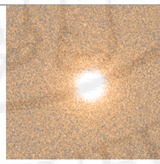	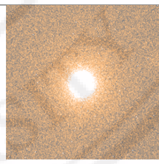	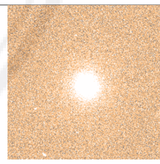
5	NGC 4060	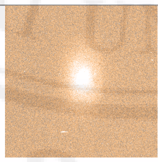	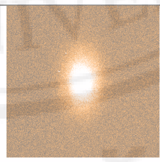	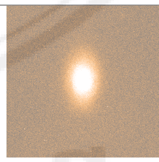	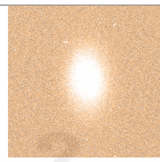
6	NGC 4056	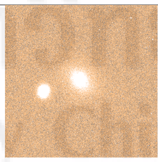	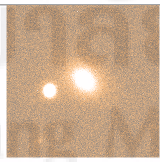	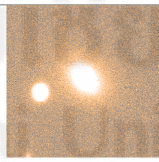	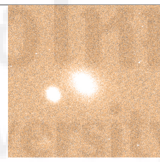
7	NGC 4065	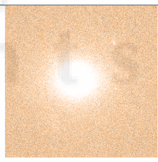	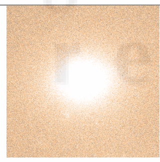	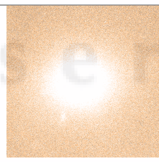	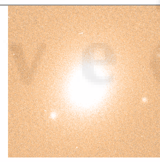

Table A.2: Sample images of the galaxies in NGC 4065 group in B, V, R_C and [SII] filters (continue I)

No.	Name	*B*	*V*	R_c	SII
8	J12040495	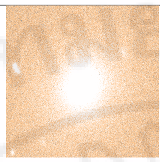	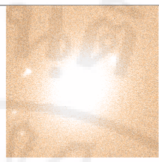	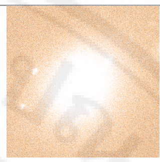	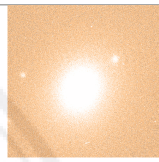
9	NGC 4061	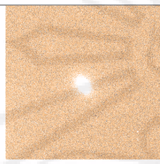	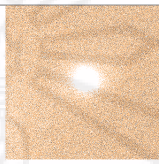	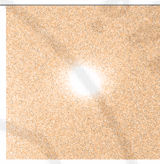	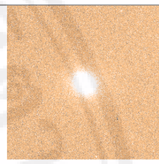
10	NGC 4072	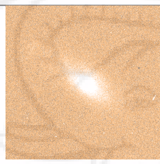	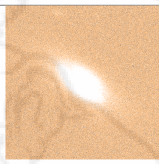	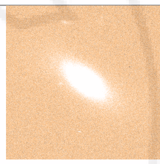	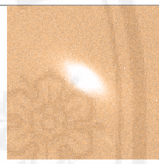
11 & 12	UGC 07049	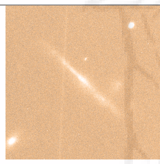	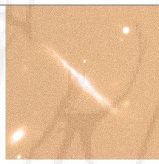	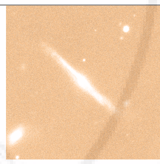	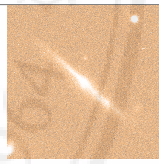
13 & 14	J12043987	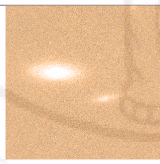	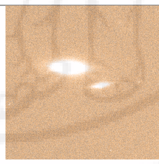	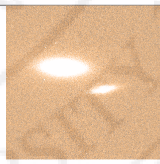	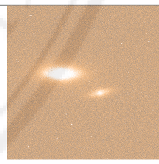
15	NGC 4076	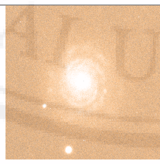	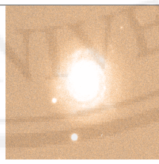	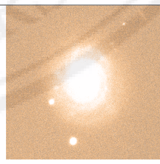	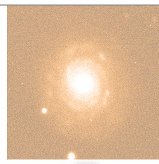
16	J120425.68	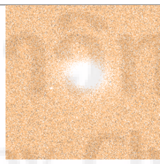	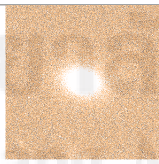	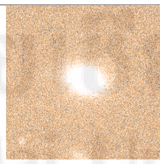	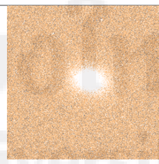
17	J12042275	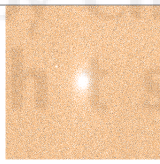	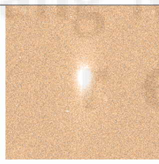	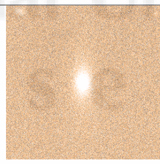	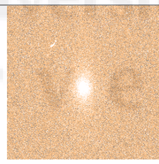

Table A.3: Sample images of the galaxies in NGC 4065 group in B, V, R_C and [SII] filters (continue II)

No.	Name	*B*	*V*	R_c	SII
18	J12035600	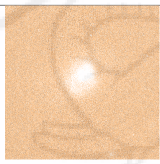	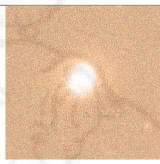	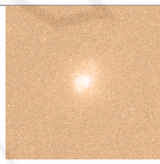	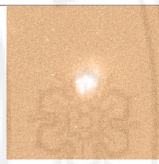
19	J12034825	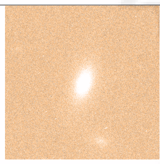	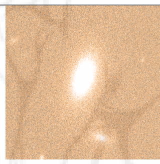	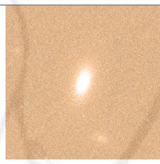	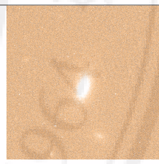
20	J12035132	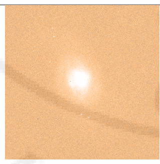	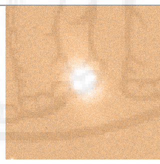	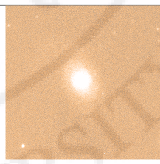	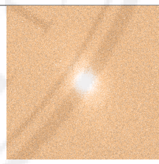
21	J12032530	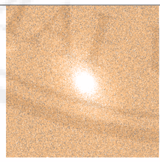	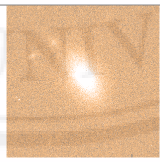	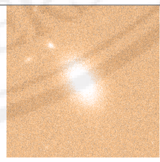	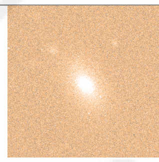

Appendix B

Publication & Conferences

B.1 APRIM 2014

PUBLICATIONS OF THE KOREAN ASTRONOMICAL SOCIETY
30: 465 ~ 467, 2015 September

pISSN: 1225-1534
eISSN: 2287-6936
http://dx.doi.org/10.5303/PKAS.2015.30.2.465

INTERACTIONS BETWEEN GALAXIES IN A LOW-REDSHIFT GROUP: THE NGC 4065 GROUP

ORARIK TASUYA[1], UTANE SAWANGWIT[2], AND WICHEAN KRIWATTANAWONG[1]
[1]Department of Physics and Materials Science, Faculty of Science, Chiang Mai University, Chiang Mai 50200, Thailand
[2]National Astronomical Research Institute of Thailand, Chiang Mai 50200, Thailand
E-mail: t.orarik@gmail.com, k.wichean@gmail.com
(Received November 30, 2014; Reviced May 31, 2015; Aaccepted June 30, 2015)

ABSTRACT

We presents a study of interactions between galaxies in the low-redshift group known as the NGC 4065 group. Imaging data were taken using the 2.4 meter telescope at the Thai National Observatory (TNO) for B, V and R_c broadband filters and [S II] and Red-continuum narrowband filters. There are 21 galaxies in our sample. The results show that most early type galaxies (ETGs) with equivalent width $EW(\mathrm{H}\alpha) <$ 10 Å are gas-deficient galaxies, while late type galaxies (LTGs) show more $EW(\mathrm{H}\alpha)$ and are bluer than the ETGs. This means that star formation activity in the LTGs could be triggered by tidal interactions between galaxy members due to dense environmental effects in the compact group.

Key words: galaxies: interactions – galaxies: star formation – galaxies: groups: individual (NGC 4065)

1. INTRODUCTION

The data for this research were taken using a 2.4 meter Ritchey-Chretien, alt-azimuth drive reflecting telescope at the Thai National Observatory (TNO) on 25–27 February and 9–11 March, 2014. Ten pointing observations were done, using a U-42 Apogee CCD with exposure times of 900 s, 600 s and 300 s for $BV R_c$ broadband and 900 s for both [S II] and red-continuum narrowband filter systems, respectively. The targets are sample galaxies in a low-redshift group, the NGC 4065 group. Twenty-one galaxies were confirmed to be members in this group by redshifts collected from the NASA/IPAC Extragalactic Database (NED).

2. METHODOLOGY

The diameter of the galaxies in the sample were taken to be the B_{25} isophotes, with an ellipse fitting of the galaxy profile perofrmed using ESP-ELLPRO (a package of Starlink software). ESP-ELLPRO produces three parameters for the fits, i.e., the ellipticity (e), semi-major axis (a_{25}) and position angle (PA). Then, the B_{25} diameter was applied to measure B, V and R magnitudes and flux counts for the red-continuum and [S II] filters.

The galaxy morphology of the sample in this research was classified following the de Vaucouleurs classification and T-Type systems. We found that most of our sample are ETGs; ten elliptical, six lenticular and five spiral galaxies. Of these spiral types, three of them are peculiar galaxies. We also found one radio galaxy and two galaxies with active galactic nucleus (AGN).

The equivalent width of Hα, $EW(\mathrm{H}\alpha)$, a parameter corresponding to star formation activity, was obtained by subtracting the red-continuum flux count from the [S II] narrowband flux count, and using the following equation (Gavazzi et al., 2006; Kriwattanawong et al., 2011):

$$EW(\mathrm{H}\alpha) = \frac{\int T_n(\lambda)\, d\lambda}{T_n(6563\,(1+z))} \frac{C_{\mathrm{H}\alpha}}{C_c} \qquad (1)$$

where $T_n(\lambda)$ is the throughput of the [S II] filter band, z is the redshift of the galaxy, $C_{\mathrm{H}\alpha}$ is the continuum subtracted Hα signal count within the B_{25} diameter, and C_c is the continuum signal count within the B_{25} diameter.

3. RESULTS

The results show that the $B-R$ color of our sample varies from 0.9 to 1.4, while the M_B magnitude is scattered over a wide range without correlation with the color index, as shown in Figure 1.

The plot of the $B-R$ color vs T-Type in Figure 2 shows that the LTGs of our sample tend to be bluer than the ETGs, except for the radio galaxy and two galaxies with AGN. This is the cause of the widely scattered colors for the late type subsample.

The plot of $EW(\mathrm{H}\alpha)$ vs T-Type in Figure 3 shows that the LTGs tend to have higher $EW(\mathrm{H}\alpha)$ than the ETGs. Particularly, the radio galaxy exhibits the highest star formation activity. All late type and two of the S0 type galaxies show high star formation ($EW(\mathrm{H}\alpha) >$ 10 Å), whereas the other early type sample was found to have $EW(\mathrm{H}\alpha)$ with scattered values lower than 10 Å.

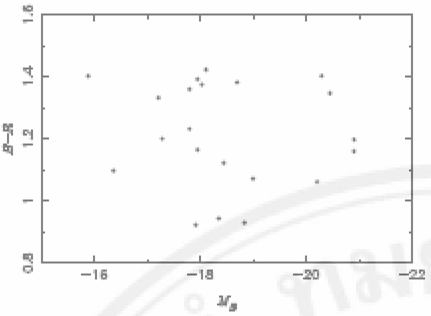

Figure 1. The plot between $B-R$ color and absolute magnitude M_B

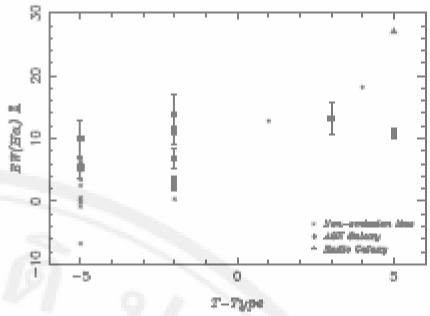

Figure 3. The plot between $EW(H\alpha)$ and $T-Type$. Crosses represent galaxies with S/N of $EW(H\alpha) < 3$, whereas the others are emission line galaxies.

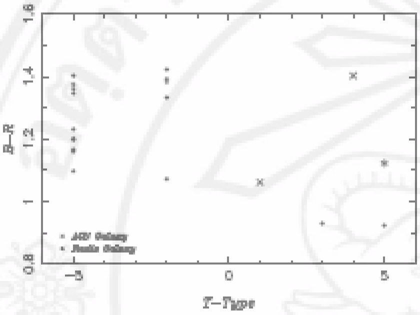

Figure 2. The plot between $B-R$ color and $T-Type$ with marked symbols for the radio galaxy (asterisk) and AGN (cross)

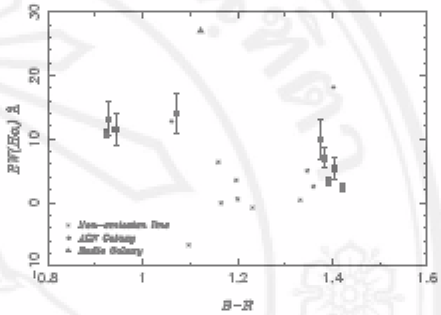

Figure 4. The plot between $EW(H\alpha)$ and $B-R$ color.

Figure 4 illustrates a diagram of $EW(\mathrm{H}\alpha)$ versus the $B-R$ color. It was found that for emission line galaxies, the bluer galaxies tend to have higher $EW(\mathrm{H}\alpha)$ than the ETGs. All LTGs, including 3 active galaxies, and blue ETGs with $B-R$ less than 1.1 show ongoing high star formation rates ($EW(\mathrm{H}\alpha) > 10$ Å).

4. CONCLUSIONS

Studying a sample of galaxies in the low-redshift compact group NGC 4065, we find that the ETGs seem to be redder than the LTGs. All LTGs and two blue lenticular galaxies show ongoing high star formation rates, whereas the others are ETGs with $EW(\mathrm{H}\alpha)$ less than 10 Å or no emission line. We know the ETGs have a lower star formation rate than the LTGs because of insufficient gas material to produce star formation (Haynes & Giovanell., 1984). However, some of the ETGs sample show high star formation rates even though they are not in dense H I regions (Freeland et al., 2009) which are abundant in hydrogen to produce star formation. Freeland et al. (2010) found evidence of ram pressure and tidal interaction in a star-forming galaxy, UGC 7049, one of our sample galaxies. These results indicate that most of the ETGs in this compact group are gas-deficient galaxies, while rich-gas LTGs could be affected by a dense environment. The formation of young massive stars might be triggered by tidal interactions among galaxy members (Boselli et al., 2006; Moss., 2006) and cause the emission line galaxies to have bluer colors than the passive ETGs.

ACKNOWLEDGMENTS

We gratefully acknowledge financial support for this research, which was provided by the National Research Council of Thailand (NRCT), the National Astronomical Research Institute of Thailand (NARIT) and the Development and Promotion of Science and Technology Talents Project (DPST). This research has made use of the NASA/IPAC Extragalactic Database (NED).

REFERENCES

Boselli, A. & Gavazzi, G., 2006, Environmental Effects on Late-Type Galaxies in Nearby Clusters, PASP, 118, 517

Freeland, E., Stilp, A., & Wilcots, E. 2009, H I Observations of Five Groups of Galaxies, ApJ, 138, 295

Freeland, E., Sengupta C., & Croston J. H., 2010, Quantifying the Importance of Ram-Pressure Stripping in a Galaxy Group at 100 Mpc, MNRAS, 409, 1518

Gavazzi, G., Boselli, A., Cortese L., Arosio, I., Gallazzi, A., Pedotti, P., & Carrasco, L., 2006, Hα Surface Photometry in Nearby Clusters, A&A, 446, 839

Haynes, M. P. & Giovanell, R., 1984, Neutral Hydrogen in Isolated Galaxies. IV - Results for the Arecibo Sample, ApJ, 89, 758

Kriwattanawong. W., Moss. C., James. P. A., & Carter D.,

2011, The Galaxy Population of Abell 1367: Photometric and Spectroscopic Data, A&A, 527, A101
Moss, C., 2006, Enhanced Mergers of Galaxies in Low-redshift Cluster, MNRAS, 373, 167

B.2 SPC 2015

Star Formation, Stellar Age and Metallicity in a Galaxy Group NGC 4065

O. Tasuya[1*], W. Kriwattanawong[1] and U. Sawangwit[2]

[1]*Department of Physics and Materials Science, Faculty of Science, Chiang Mai University, Chiang Mai, 50200 Thailand*
[2]*National Astronomical Research Institute of Thailand, Chiang Mai, 50200 Thailand*
**Corresponding author. E-mail: t.orarik@gmail.com*

Abstract

We present a study of star formation, mean stellar age and metallicity, and interactions between galaxies in a low-redshift group, NGC 4065 group. Data Observations for B, V and R_C broadband filters and [S II] and Red-continuum narrowband were carried out on the 2.4 meter telescope at Thai National Observatory (TNO). There are 21 galaxies in our sample. The amount of star formation activity is represented by the equivalent width of hydrogen alpha (EW(Hα)). Mean stellar luminosity-weighted age and metallicity were examined by using the stellar population synthesis model of Vazdekis et al. (2010) and infrared magnitudes from GOLDMINE database via B-J vs J-K diagram. The result shows that most of early type galaxies (ETGs) in the sample has EW(Hα) less than 10 Å, meaning to be gas-deficient galaxies. While late type galaxies (LTGs) show more EW(Hα) and bluer than the ETGs. Mean stellar age and metallicity can be interpreted using the color-color diagram but not very clearly. Most of our sample is inclined to have high metallicity, whereas mean stellar age is unidentifiable. That means star formation activity in the LTGs could be triggered by ram-pressure stripping and tidal interaction between galaxy members due to dense environmental effect in the compact group.

Keywords: galaxies: interactions - galaxies: star formation - galaxies: groups: individual (NGC 4065)

Introduction

The data of this research were taken by using a 2.4 meter Ritchey-Chretien, alt-azimuth drive reflecting telescope at Thai National Observatory (TNO) on 25 - 27 February and 9 - 11 March, 2014. Ten pointing observations were done, using U-42 Apogee CCD with exposure time of 900 s, 600 s and 300 s for BVR_C broadband and 900 s for both [S II] and Red-continuum narrowband filter systems, respectively. The targets are sample galaxies in a low-redshift group, called NGC 4065 group. Twenty-one galaxies were confirmed to be members in this group by redshift, collected from the NASA/IPAC Extragalactic Database (NED).

Materials and Methods

B_{25} diameter

Diameter of the galaxy sample was determined at B_{25} isophotes, which performed an ellipse fitting galaxy profile, by using ESP-ELLPRO (a package of Starlink software). The ESP-ELLPRO provided three parameters of the diameter, i.e., ellipticity *(e)*, semi-major axis (a_{25}) and position angle *(PA)*. Then, the B_{25} diameter was applied to measure *B*, *V* and *R* magnitudes and flux counts for Red-continuum and [S II] filter.

Galaxy morphological classification

The galaxy morphology of the sample in this research was classified following the de Vaucouleurs classification and T-Type systems. We found that most of our sample is the ETGs; ten elliptical, six lenticular and five spiral galaxies. Of these spiral types, three of them are peculiar galaxies. There were also found one radio galaxy and two galaxies with active galactic nucleus (AGN).

Equivalent width of Hα

Equivalent width of Hα, *EW*(Hα), a parameter corresponding to star formation activity, was obtained by subtracting Red-continuum flux count out of [S II] narrowband flux count, and then calculating by using the following equation (Gavazzi et al., 2006; Kriwattanawong et al., 2011)

$$EW(H\alpha) = \frac{\int T_n(\lambda)d\lambda}{T_n(6563(1+z))} \times \frac{C_{H\alpha}}{C_C} \qquad (1)$$

Where

$T_n(\lambda)$ is throughput of [S II] filter band.

z is red-shift of galaxy.

$C_{H\alpha}$ is continuum subtracted **H**α signal count within the B_{25} diameter.

C_C is continuum signal count within the B_{25} diameter.

Mean stellar age and metallicity

Typically, mean stellar luminosity-weighted age and metallicity can be estimated by using colors of galaxy. The galaxy's colors become bluer follows amount of young massive stars, which are typically blue. These young stars could collect heavy element from remnant of previous generation via supernova process, and thus young stars can be expected to be have higher metallicity than the old ones.

To predict the mean stellar luminosity-weighted age and metallicity, we created the optical/infrared color-color (B-J vs J-K) diagram using the stellar population synthesis model of Vazdekis et al. (2010). Infrared magnitudes were collected from GOLDMINE database.

Results and Discussion

Color and magnitude

The result shows that *B-R* color of our sample vary in a range of 0.9 to 1.4. While, M_B magnitude scatters in a wide range without correlation with the color index as shown in Figure 1.

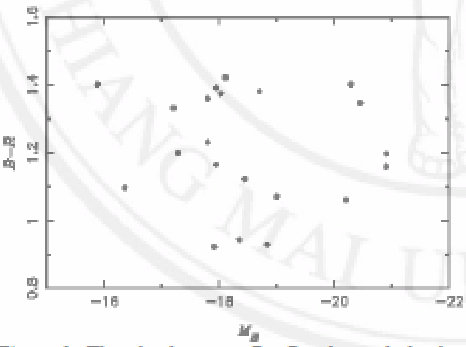

Figure 1. The plot between *B* - *R* color and absolute magnitude M_B

Color and T-Type

The plot between *B-R* color and T-Type in Figure 2 shows that LTGs of our sample tend to be bluer than ETGs, except the radio galaxy and two galaxies with AGN. This is a cause of widely scattered colors for the late type subsample.

EW(Hα) and T-Type

The plot between *EW*(Hα) and *T-Type* in Figure 3 shows that the LTGs tend to have *EW*(Hα) than the ETGs. Particularly, the radio galaxy exhibits highest star formation activity. All late type and two S0 type galaxies show high star formation *EW*(Hα) > 10 Å, whereas the other early type sample was found to have *EW*(Hα), scattered lower than 10 Å.

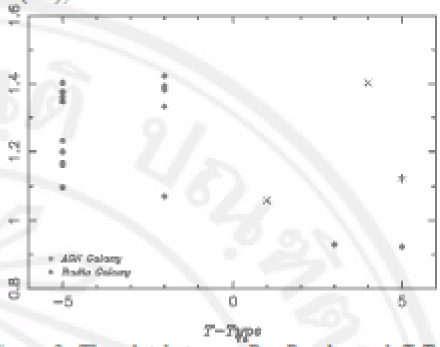

Figure 2. The plot between *B* - *R* color and *T-Type* with marked symbols for the radio galaxy (asterisk) and AGN (cross).

EW(Hα) and color

Figure 4 illustrates a diagram of *EW*(Hα) versus *B-R* color. It is found that for emission line galaxies, the bluer galaxies tend to have higher *EW*(Hα) than the ETGs. All LTGs, including 3 active galaxies and blue ETGs with *B-R* less than 1.1 are ongoing high star formation *EW*(Hα) > 10 Å.

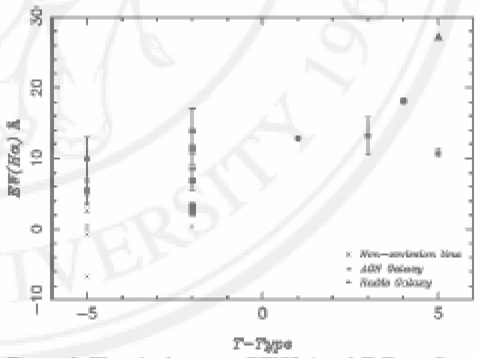

Figure 3. The plot between *EW*(Hα) and *T-Type*. Cross represents galaxies with S/N of *EW*(Hα) < 3, whereas the others are emission line galaxies.

Estimate of mean stellar age and metallicity

The estimate of mean stellar luminosity-weighted age and metallicity using color-color diagram is shown in Figure 5. Unfortunately, for our galaxy sample, both B-K and J-K colors do not fit with the model grid. From this result, we only illustrates that the most of our galaxy tends to have the high metallicity. There may be only two metal poor galaxies. While mean stellar age is hard to be determined.

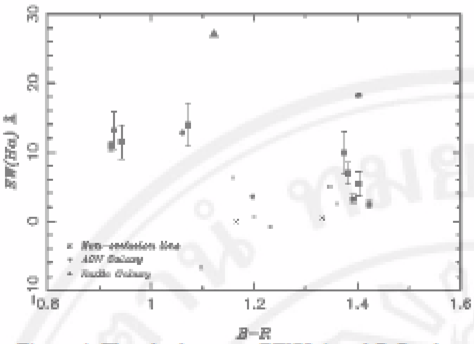

Figure 4. The plot between EW(Hα) and B-R color.

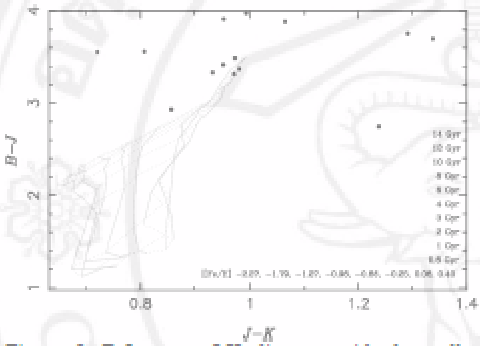

Figure 5. B-J versus J-K diagram with the stellar population synthesis model for the metallicity from -2.27 to 0.4 and the age from 0.6 Gyr to 14 Gyr.

Conclusions

Studying through 21 sample galaxies in the low-redshift compact group NGC 4065, we find that the ETGs seem to be redder than the LTGs. All LTGs and two blue lenticular galaxies are ongoing high star formation, whereas the others are ETGs with EW(Hα) less than 10 Å or non-emission line. All sample galaxies tend to have high metallicity, only two ETGs are metal poor galaxies. The mean stellar age is unable to be identified due to unfitted with the model grid. Typically, the ETGs usually have less star formation than the LTGs because of insufficient gas material to produce star formation (Haynes & Giovanell., 1984). But some of the ETGs in our sample shows high EW(Hα) even there are not in the dense H I region (Freeland et al., 2009) which is full of hydrogen abundance to produce star formation, while Freeland et al. (2010) found the evidence of ram pressure and tidal interaction in a star-forming galaxy, UGC 7049, one of our sample galaxy. The results indicate that most of the ETGs in this compact group are gas-deficient galaxies, whereas rich-gas LTGs could be affected by dense environment. Young massive stars might be triggered by tidal interaction among galaxy members (Boselli et al., 2006; Moss., 2006) and caused bluer colors of those emission line galaxies, than the passive ETGs.

Acknowledgments

We gratefully acknowledge financial support for this research, which was provided by the National Research Council of Thailand (NRCT), the National Astronomical Research Institute of Thailand (NARIT) and the Development and Promotion of Science and Technology Talents Project (DPST). This research has made use of the NASA/IPAC Extragalactic and GOLDMINE database.

References

1. A. Boselli and G. Gavazzi, "Environmental Effects on Late-Type Galaxies in Nearby Clusters", PASP **118** (2006) 517.
2. E. Freeland, A. Stilp and E. Wilcots, "H I Observations of Five Groups of Galaxies", ApJ 138 (2009) 295.
3. E. Freeland, C. Sengupta and J. H. Croston, "Quantifying the Importance of Ram-Pressure Stripping in a Galaxy Group at 100 Mpc", MNRAS **409** (2010) 1518.
4. G. Gavazzi, A. Boselli, L. Cortese, I. Arosio, A. Gallazzi, P. Pedotti and L. Carrasco, "Hα Surface Photometry in Nearby Clusters", A&A **446** (2006) 839.
5. M. P. Haynes and R. Giovanell, "Neutral Hydrogen in Isolated Galaxies. IV-Results for the Arecibo Sample", ApJ, 89 (1984) 758.
6. R. Saito, G. Dresselhaus, and M. S. Dresselhaus, "Physical Properties of Carbon Nanotubes", London, Imperial College Press, 1998.
7. W. Kriwattanawong, C. Moss, P. A. James and D. Carter, "The Galaxy Population of Abell 1367: Photometric and Spectroscopic Data", A&A **527** (2011) A101.
8. C. Moss, "Enhanced Mergers of Galaxies in Low-redshift Cluster", MNRAS 373 (2006) 167.
9. A. Vazdekis, P. Sánchez-Blázquez, J. Falcón-Barroso, A. J. Cenarro, M. A. Beasley, N. Cardiel, J. Gorgas, R. F. Peletire, "Evolutionary stellar population synthesis with MILES - I. The base models and a new line index system", MNRAS **404** (2010) 1639.

Curriculum Vitae

Name-Surname	Mr. Orarik Tasuya
Date of Birth	18 March 1990
Education	
2013 - 2016	Master of Science (Physics), Department of Physics and Materials Science, Faculty of Science, Chiang Mai University, Thailand
2009 - 2012	Bachelor of Science (Physics), Department of Physics and Materials Science, Faculty of Science, Chiang Mai University, Thailand
2006 - 2008	High School Diploma (Science and Mathematics Program), Yupparaj Wittayalai School, Chiang Mai, Thailand
Publication	O. Tasuya, W. Kriwattanawong and U. Sawangwit, "Interactions Between Galaxies in a Low-Redshift Group: the NGC 4065 Group", Publications of The Korean Astronomical Society, 30, 465-467